On the Computation of EXIT Characteristics for Symbol-Based Iterative Decoding

Jörg Kliewer[1], Soon Xin Ng[2], and Lajos Hanzo[2]

[1]University of Notre Dame, Department of Electrical Engineering, Notre Dame, IN 46556, U.S.A.,
e-mail: jkliewer@nd.edu

[2]University of Southampton, Communications Research Group, Southampton, SO17 1BJ, U.K.,
e-mail: {sxn,lh}@ecs.soton.ac.uk

Abstract

In this contribution we propose an efficient method for computing symbol-based extrinsic information transfer (EXIT) charts, which are useful for estimating the convergence properties of non-binary iterative decoding. A standard solution is to apply *a priori* reliability information to the *a posteriori* probability (APP) constituent decoder and compute the resultant average extrinsic information at the decoder's output using multidimensional histogram measurements. However, the employment of this technique is only feasible for a low number of bits per symbol, since the complexity of this approach increases exponentially with the number of bits per symbol. We demonstrate that by averaging over a function of the extrinsic APPs for a long block the extrinsic information can be estimated at a low complexity. In contrast to using histogram measurements, the proposed technique allows us to generate EXIT charts even for a high number of bits per symbol. Our design examples using either a non-binary serial concatenated code or turbo trellis-coded modulation demonstrate the attractive benefits of the proposed approach.

1 Introduction

Extrinsic information transfer (EXIT) charts have recently emerged as useful tools designed for analyzing the convergence properties of iteratively decoded concatenated coding schemes and for assessing the overall performance of the underlying transmission system [1], [2]. Their accuracy is particularly impressive, when the interleaver block-length tends to infinity. A substantial advantage of EXIT charts is that convergence of the entire decoding scheme can be evaluated *without* performing time-consuming decoder simulations. We will demonstrate that EXIT charts can be used for finding powerful non-binary codes with guaranteed convergence for a given channel Signal-to-Noise Ratio (SNR). Specifically, codes capable of approaching the channel capacity have been successfully designed by applying an EXIT-chart-based analysis [3], [4].

The standard method of calculating EXIT characteristics is to evaluate the histogram of the decoder's extrinsic soft output, followed by a numerical integration in order to determine the extrinsic mutual information. When the EXIT characteristics of two (or more) constituent decoders are plotted within the same diagram, the transfer of extrinsic information between the decoders can be visualized. However, in case of non-binary codes the histogram computation becomes prohibitively complex even for a moderate number of bits per symbol. This is due to the fact that the soft values which are exchanged between the constituent decoders of an iterative decoding scheme no longer consist of a single scalar value as in the binary scenario. Instead, they are now represented by a vector of (logarithmic) probabilities for all non-binary symbols constituting the signaling alphabet. Thus, multidimensional histograms have to be determined for all vector entries, followed by a multidimensional integration over each element of the probability vector. Unfortunately, both the number of histograms and integral dimensions to be evaluated increase exponentially with the number of bits per symbol.

Non-binary EXIT charts have been introduced in [5], where serially concatenated systems constituted by an inner trellis-coded modulation (TCM) and outer space-time convolutional code have been analyzed. Recently, in [6] this approach was applied to turbo TCM (TTCM) [7]. However, all these approaches are histogram-based and thus are only suitable for non-binary symbols constituted by at most two or three bits. By contrast, we propose an efficient technique of computing non-binary EXIT charts from symbol-based *a posteriori* probabilities (APPs). The proposed technique represents a generalization of the approach presented in [8] for a binary scenario. It is based on the fact that the symbol-based APPs generated at the output of a SISO decoder represents a sufficient statistic for the channel observations at its input. As an advantage, the symbol-based extrinsic mutual information can be computed at a considerably reduced complexity

This work was partly supported by the German Research Foundation (DFG), by EPSRC, Swindon, U.K., and by the EU under the auspices of the PHOENIX and NEWCOM projects.

compared to the histogram-based approaches. The proposed method is well suited for the analysis of non-binary iterative decoding schemes designed for a high number of bits per symbol, i.e., for a large signaling alphabet. Design examples will be provided for a non-binary serially concatenated bit-interleaved coded modulation (BICM) scheme and a TTCM arrangement, both employing a 16-QAM signaling alphabet.

The outline of the paper is as follows. In Section 2 our notations and decoding model are introduced, while Sections 3 and 4 describe the non-binary EXIT-chart generation technique proposed. Our design examples are discussed in Section 5 and the paper is concluded in Section 6.

2 Notations and decoding model

Random variables (r.v.s) are denoted with capital letters and their corresponding realizations with lower case letters. Sequences of random variables and their realizations are indicated by boldface italics letters (as "$\boldsymbol{U}$" or "$\boldsymbol{u}$"). Furthermore, boldface roman letters denote vectors (as "$\mathbf{E}$" or "$\mathbf{e}$"). The symbol index is denoted by "k" and the bit-index by "ℓ".

The decoding model utilized in this paper is depicted in Fig. 1 [2]. For the iterative decoding of an outer code in a serial concatenated scheme, the connections marked with "1" are active in Fig. 1 and the communication channel is not present or completely corrupted. All other scenarios for iterative decoding (inner serially concatenated code and parallel concatenation) have a constituent decoder modeled by Fig. 1 with the switches in position "2". In Fig. 1 the stationary input symbol sequence $\boldsymbol{U} = [U_1, U_2, \ldots, U_k, \ldots]$ consists of r.v.s U_k, where the corresponding realizations u_k have M bits / symbol and are taken from a finite signaling alphabet $\mathcal{U} = \{0, 1, \ldots, 2^M - 1\}$. For each symbol a channel code $\mathcal{C}$ having a rate of $R = M/N$ generates an N-bit encoded symbol X_k, which leads to the sequence $\boldsymbol{X} = [X_1, X_2, \ldots, X_k, \ldots]$ transmitted over the communication channel. The sequence $\boldsymbol{Y}$ is finally observed at the channel's output.

The *a priori* channel models the *a priori* information used at the constituent decoders. The input sequence $\boldsymbol{V} = [V_1, V_2, \ldots, V_k, \ldots]$ has realizations v_k from the alphabet $\mathcal{V} = \{0, 1, \ldots, 2^K - 1\}$ where $K = N$ if the switches in Fig. 1 are in position "1" (i.e., in the case of an outer decoder for serial concatenation) and $K = M$ otherwise. Thus, each v_k comprises K bits $v_{k,\ell}$, $\ell \in \{1, 2, \ldots, K\}$. For the output sequence $\boldsymbol{W}$ the same considerations hold as for the output $\boldsymbol{Y}$ of the communication channel. Furthermore, the vector sequence $\boldsymbol{A} = [\mathbf{A}_1, \mathbf{A}_2, \ldots, \mathbf{A}_k, \ldots]$ contains the *a priori* information in form of conditional probability density functions (pdfs) with the vector-valued r.v.s $\mathbf{A}_k$ having the realizations

$$\mathbf{a}_k = [p(w_k|V_k = 0), p(w_k|V_k = 1), \ldots, p(w_k|V_k = 2^K - 1)]. \quad (1)$$

The SISO decoder then employs both the output of the communication and the *a priori* channel for computing both the *a posteriori* information $\boldsymbol{D} = [\mathbf{D}_1, \mathbf{D}_2, \ldots, \mathbf{D}_k, \ldots]$ and the extrinsic information $\boldsymbol{E} = [\mathbf{E}_1, \mathbf{E}_2, \ldots, \mathbf{E}_k, \ldots]$ [9]. The latter is then used as *a priori* information for the other constituent decoder. The sequence $\boldsymbol{D}$ comprises the r.v.s $\mathbf{D}_k$ and has the following realizations

$$\mathbf{d}_k = [P(U_k = 0|\boldsymbol{y}, \boldsymbol{w}), P(U_k = 1|\boldsymbol{y}, \boldsymbol{w}), \ldots, P(U_k = 2^M - 1|\boldsymbol{y}, \boldsymbol{w})], \quad (2)$$

where $P(U_k = u_k|\boldsymbol{y}, \boldsymbol{w})$ represents the *a posteriori* probabilities (APPs) for the source hypothesis $U_k = u_k$. The extrinsic sequence $\boldsymbol{E}$ is described by the r.v.s $\mathbf{E}_k$ with

$$\mathbf{e}_k = [P(V_k = 0|\boldsymbol{y}, \boldsymbol{w}_{[k]}), P(V_k = 1|\boldsymbol{y}, \boldsymbol{w}_{[k]}), \ldots, P(V_k = 2^K - 1|\boldsymbol{y}, \boldsymbol{w}_{[k]})], \quad (3)$$

where the notation $\boldsymbol{w}_{[k]}$ denotes that the entry corresponding to the symbol instant k is excluded from the sequence $\boldsymbol{w}$.

3 Symbol-based EXIT charts

EXIT charts visualize the input / output characteristics of the constituent SISO decoders in terms of a mutual information transfer between the sequence $\boldsymbol{V}$ and *a priori* information $\boldsymbol{A}$ at the input of the decoder, as well as between $\boldsymbol{V}$ and $\boldsymbol{E}$ at the output, respectively. In the following we summarize the calculation of non-binary EXIT charts, which are essentially a straightforward extension of the binary case [1], [2], [10].

Denoting the mutual information between two r.v.s X and Y as $I(X;Y)$, for a given length Q of the sequence $\boldsymbol{V}$ we have

$$I_A := \frac{1}{Q}\sum_{k=1}^{Q} I(V_k; \mathbf{A}_k), \quad I_E := \frac{1}{Q}\sum_{k=1}^{Q} I(V_k; \mathbf{E}_k). \quad (4)$$

Herein, I_A represents the average *a priori* information and I_E the average extrinsic information, respectively. Note that these quantities are defined as approximations of the sequence-wise mutual information per symbol $1/Q \cdot I(\boldsymbol{V}; \boldsymbol{A})$ and $1/Q \cdot I(\boldsymbol{V}; \boldsymbol{E})$, respectively. The transfer characteristic (or function) T of the constituent decoder is given as $I_E = T(I_A, \rho)$, where ρ represents a quality parameter of the communication channel. For example, ρ may represent the noise variance of an AWGN channel. In the case of an outer decoder in a serially concatenated scheme T does not depend on ρ. An EXIT chart can now be obtained by plotting the

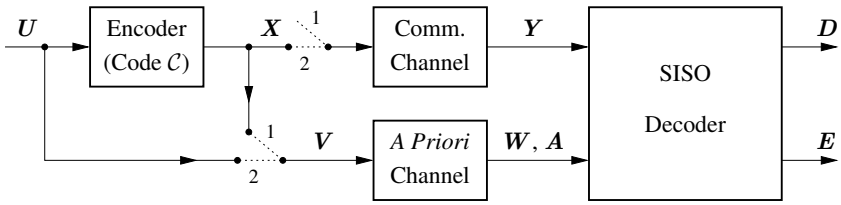

Fig. 1. Decoding model for parallel concatenation (switches in position "1") and an inner / outer code in a serial concatenation (switches in position "1"/"2")

transfer characteristics T for both constituent decoders within a single diagram, where the axes have to be swapped for one of the constituent decoders [1] (normally the outer one for serial concatenation).

The mutual information $I(V_k;\mathbf{A}_k)$ in (4) can be expressed as

$$I(V_k;\mathbf{A}_k) = \sum_{v_k=0}^{2^K-1} \int_{\mathbf{a}_k} p(\mathbf{a}_k|v_k)\,P(v_k)\cdot \log_2\left(\frac{p(\mathbf{a}_k|v_k)}{p(\mathbf{a}_k)}\right) d\mathbf{a}_k \quad (5)$$

where we have

$$p(\mathbf{a}_k) = \sum_{v_k=0}^{2^K-1} p(\mathbf{a}_k|v_k)\,P(v_k) \quad (6)$$

and the *a priori* probabilities $P(v_k)$ for the symbols v_k. The 2^K-dimensional integration in (5) can be evaluated numerically, where the pdf $p(\mathbf{a}_k|v_k)$ in many cases can be obtained analytically (e.g., for the AWGN channel [1]). Likewise, we can write $I(V_k;\mathbf{E}_k)$ as

$$I(V_k;\mathbf{E}_k) = \sum_{v_k=0}^{2^K-1} \int_{\mathbf{e}_k} p(\mathbf{e}_k|v_k)\,P(v_k)\cdot \log_2\left(\frac{p(\mathbf{e}_k|v_k)}{p(\mathbf{e}_k)}\right) d\mathbf{e}_k \quad (7)$$

with the pdf $p(\mathbf{e}_k)$ written in the same manner as in (6), where $\mathbf{a}_k$ is replaced by $\mathbf{e}_k$. The standard approach to determine $p(\mathbf{e}_k|v_k)$ is by computing a 2^K-dimensional histogram for each symbol hypothesis $v_k \in \mathcal{V}$ [1], [5], [6] which in practice is exceedingly difficult to compute for $K \geq 3$. Furthermore, the evaluation of the 2^K-dimensional integral in (5) becomes excessive for symbol lengths K having a couple of bits. In fact, for a discretization of the integrals with L points corresponding to a certain interval of the logarithmic vector elements[1] in $\mathbf{a}_k$ and $\mathbf{e}_k$ (say, e.g., $[-20, 0]$) we have to sum over L^{2^K} discrete numbers. The calculation of the mutual information for $K = 3$ bits and $L = 100$ points (which should be sufficient according to our experiments) involves a summation over 10^{16} elements.

[1] Instead of using the pdfs / probability mass functions in both $\mathbf{a}_k$ and $\mathbf{e}_k$ directly, the logarithm of these quantities is employed due to numerical reasons. However, this does not change the value of $I(V_k;\mathbf{A}_k)$ and $I(V_k;\mathbf{E}_k)$.

By contrast, for $K = 4$ this number increases to 10^{32} elements. Therefore, the calculation of a symbol-based transfer function is computationally feasible only for two-bit symbols without loosing the computational advantage of an EXIT-chart based design compared to a full decoder simulation. In the next section we will present a more effective way of computing the symbol-based transfer characteristics, which is suitable also for larger signaling alphabets.

4 Efficient computation of symbol-based EXIT transfer functions

As a starting point let us consider the following lemma.

Lemma 1. *Let* $\mathbf{e}_k$ *be defined as in* (3)*. Then, for all values* $v_k \in \mathcal{V}$ *we have* $P(v_k|\mathbf{e}_k) = P(v_k|\boldsymbol{y}, \boldsymbol{w}_{[k]})$.

Proof. The proof can be carried out as a modification of the binary case described in [8]. The conditional pdf of $\mathbf{e}_k$ with respect to the symbol v_k can be expressed with the conditional pdf $p(\boldsymbol{y}, \boldsymbol{w}_{[k]}|V_k = v_k)$ as

$$p(\mathbf{e}_k|V_k = v_k) = \int_{\boldsymbol{y},\boldsymbol{w}_{[k]}:\mathbf{e}_k} p(\boldsymbol{y}, \boldsymbol{w}_{[k]}|V_k = v_k)\,d\boldsymbol{y}\,d\boldsymbol{w}_{[k]}, \quad (8)$$

where the notation "$\boldsymbol{y}, \boldsymbol{w}_{[k]} : \mathbf{e}_k$" means that for a *given* $\mathbf{e}_k$ value the integration is carried out over the whole set given by

$$\{\boldsymbol{y}, \boldsymbol{w}_{[k]} : [P(V_k = 0|\boldsymbol{y}, \boldsymbol{w}_{[k]}), P(V_k = 1|\boldsymbol{y}, \boldsymbol{w}_{[k]}), \ldots, P(V_k = 2^K - 1|\boldsymbol{y}, \boldsymbol{w}_{[k]})] \stackrel{!}{=} \mathbf{e}_k\}. \quad (9)$$

By applying Bayes' theorem and by using the definition $e_{k,\lambda} := P(V_k = \lambda|\boldsymbol{y}, \boldsymbol{w}_{[k]})$, $\lambda \in \mathcal{V}$, from (8) we obtain for the λ-th entry of the vector $\mathbf{e}_k$

$$p(\mathbf{e}_k|V_k = \lambda) = \frac{e_{k,\lambda}}{P(V_k = \lambda)} \int_{\boldsymbol{y},\boldsymbol{w}_{[k]}:\mathbf{e}_k} p(\boldsymbol{y}, \boldsymbol{w}_{[k]})\,d\boldsymbol{y}d\boldsymbol{w}_{[k]} = \frac{e_{k,\lambda}}{P(V_k = \lambda)}\,p(\mathbf{e}_k). \quad (10)$$

A similar relation to that seen in (8) is employed for $p(\boldsymbol{y}, \boldsymbol{w}_{[k]})$, except that it is not dependent on V_k. Note that due to the condition (9) $e_{k,\lambda}$ represents a constant with respect to the integration. From (10) we obtain $P(V_k = \lambda|\mathbf{e}_k) = e_{k,\lambda} = P(V_k = \lambda|\boldsymbol{y}, \boldsymbol{w}_{[k]})$, which completes the proof for all $\lambda = v_k$, $v_k \in \mathcal{V}$. □

We are now able to prove the following theorem, which relates the extrinsic information $\mathbf{E}_k$ at symbol instant k to the observed sequences $\boldsymbol{Y}$ and $\boldsymbol{W}$ at the input of the SISO decoder in Fig. 1.

Theorem 1. *Let the entries of the vector $\mathbf{E}_k$ represent extrinsic APPs for the realizations $v_k \in \mathcal{V}$. Then, the vector $\mathbf{E}_k$ contains the same amount of information as the sequences $\boldsymbol{Y}$ and $\boldsymbol{W}_{[k]}$. In other words, we have*

$$I(V_k; \mathbf{E}_k) = I(V_k; \boldsymbol{Y}, \boldsymbol{W}_{[k]}).$$

Proof. The mutual information expression $I(V_k; \boldsymbol{Y}, \boldsymbol{W}_{[k]})$ can be expanded as

$$\begin{aligned}
&I(V_k; \boldsymbol{Y}, \boldsymbol{W}_{[k]}) \\
&= \sum_{v_k=0}^{2^K-1} \int_{\boldsymbol{y}} \int_{\boldsymbol{w}_{[k]}} p(v_k, \boldsymbol{y}, \boldsymbol{w}_{[k]}) \cdot \\
&\qquad \log_2\left(\frac{P(v_k|\boldsymbol{y}, \boldsymbol{w}_{[k]})}{P(v_k)}\right) d\boldsymbol{y}\, d\boldsymbol{w}_{[k]} \\
&= \sum_{v_k=0}^{2^K-1} \int_{\boldsymbol{y}} \int_{\boldsymbol{w}_{[k]}} \int_{\mathbf{e}_k} p(v_k, \boldsymbol{y}, \boldsymbol{w}_{[k]}, \mathbf{e}_k) \cdot \\
&\qquad \log_2\left(\frac{P(v_k|\mathbf{e}_k)}{P(v_k)}\right) d\mathbf{e}_k\, d\boldsymbol{y}\, d\boldsymbol{w}_{[k]} \qquad (11) \\
&= \sum_{v_k=0}^{2^K-1} \int_{\mathbf{e}_k} p(v_k, \mathbf{e}_k) \log_2\left(\frac{P(v_k|\mathbf{e}_k)}{P(v_k)}\right) d\mathbf{e}_k = I(V_k; \mathbf{E}_k),
\end{aligned}$$

where (11) utilizes Lemma 1 and the definition of a marginal pdf. □

Note that Theorem 1 represents a non-binary symbol-based formulation of the well-known fact that the APPs at the output of the SISO decoder represent a sufficient statistic of the received sequences $\boldsymbol{y}$ and $\boldsymbol{w}_{[k]}$. In the following we show that Theorem 1 can be used for computing the average extrinsic information from the extrinsic APPs available at the SISO decoder output.

Theorem 2. *Let the extrinsic APP $P(v_\kappa|\boldsymbol{y}, \boldsymbol{w}_{[\kappa]})$ represent an ergodic r.v. for all values $v_\kappa \in \mathcal{V}$, and let $\boldsymbol{V}$ be a stationary symbol sequence. Then, the average extrinsic information is given by*

$$I_E = H(V_1) + \lim_{L\to\infty} \frac{1}{L} \sum_{\kappa=1}^{L} \sum_{v_\kappa=0}^{2^K-1} P(v_\kappa|\boldsymbol{y}, \boldsymbol{w}_{[\kappa]}) \cdot \log_2(P(v_\kappa|\boldsymbol{y}, \boldsymbol{w}_{[\kappa]})).$$

Proof. Combining Theorem 1 and (4) as well as using the stationarity of $\boldsymbol{V}$ we can write

$$\begin{aligned}
I_E &= \frac{1}{Q} \sum_{k=1}^{Q} I(V_k; \boldsymbol{Y}, \boldsymbol{W}_{[k]}) \\
&= H(V_1) - \underbrace{\frac{1}{Q} \sum_{k=1}^{Q} H(V_k|\boldsymbol{Y}, \boldsymbol{W}_{[k]})}_{=:A}. \qquad (12)
\end{aligned}$$

The sum over the conditional entropies denoted with A in (12) can be further expanded as

$$\begin{aligned}
A &= -\frac{1}{Q} \sum_{k=1}^{Q} \sum_{v_k=0}^{2^K-1} \int_{\boldsymbol{y}} \int_{\boldsymbol{w}_{[k]}} P(v_k|\boldsymbol{y}, \boldsymbol{w}_{[k]})\, p(\boldsymbol{y}, \boldsymbol{w}_{[k]}) \cdot \\
&\qquad \log_2(P(v_k|\boldsymbol{y}, \boldsymbol{w}_{[k]}))\, d\boldsymbol{y}\, d\boldsymbol{w}_{[k]} \\
&= -E\left\{\frac{1}{Q} \sum_{k=1}^{Q} \sum_{v_k=0}^{2^K-1} P(v_k|\boldsymbol{y}, \boldsymbol{w}_{[k]}) \log_2(P(v_k|\boldsymbol{y}, \boldsymbol{w}_{[k]}))\right\}. \qquad (13)
\end{aligned}$$

Exploiting the previously stipulated ergodicity of the extrinsic APPs and defining $L := B\,Q$, where B denotes the number of length-Q blocks to be averaged, proves the theorem for $B \to \infty$. □

The result of Theorem 2 can now be used for finite values of L to approximate the average extrinsic information I_E by simply time-averaging a function of the extrinsic APPs $P(v_\kappa|\boldsymbol{y}, \boldsymbol{w}_{[\kappa]})$ over a block of L source symbols v_κ. In order to achieve a small approximation error variance, the block length L must be reasonably large. Furthermore, the entropy $H(V_1)$ can be readily determined from the *a priori* symbol distributions $P(v_k)$. Note that Theorem 2 may also be used to calculate the average *a priori* information I_A.

5 Design examples

5.1 Symbol-based serially concatenated bit-interleaved coded modulation

As a first example, we employ the I_E approximation method suggested by Theorem 2 for designing a non-binary serial concatenated BICM-aided 16-QAM scheme, which exhibits near-channel-capacity performance for transmission over perfectly interleaved flat Rayleigh fading channels. In this approach bit-interleavers are employed for both separating the outer from the inner encoder and the inner encoder from the Gray-mapped 16-QAM modulator. Furthermore, the communication channel is a perfectly interleaved flat Rayleigh channel, and the *a priori* channel in Fig. 1 represents an AWGN channel. Symbol-based iterative decoding is carried out between the constituent decoders of the inner and outer codes, where a symbol length of $K = 3$ bits is used. In order to design such a system the outer code was fixed to Paaske's maximal minimum distance rate-$R_1 = 2/3$ non-systematic convolutional (NSC) code [11], [12] having a generator polynomial matrix $\mathbf{G} = [\mathbf{g}_1; \mathbf{g}_2]$ with $\mathbf{g}_1 = (g_{11}, g_{12}, g_{13}) = (4, 2, 6)_8$ and $\mathbf{g}_2 = (g_{21}, g_{22}, g_{23}) = (1, 4, 7)_8$ in octal form, respectively. In order to complement this outer code, a memory-3 non-binary inner code was sought for the sake of ensuring that its symbol-based EXIT characteristic recorded for the Rayleigh fading channel matches the EXIT characteristic of

the NSC outer code as closely as possible. The closest match was achieved by a rate-$R_2 = 3/4$ recursive systematic convolutional code (RSC) having feedforward $(g_1, \ldots, g_3)$ and feedback (g_r) generator polynomials of $(g_r, g_1, g_2, g_3)_8 = (11, 2, 4, 10)_8$. As pointed out earlier, a symbol-length of $K = 3$ bits becomes excessive for a code search employing a histogram-based computation method for determining the EXIT characteristics of the constituent decoders. The effective throughput of this serially concatenated NSC-RSC-16QAM BICM scheme is given by

$$\eta = R_1 \, R_2 \, \log_2(\mu) = 2 \text{ bit/s/Hz}$$

where $\mu = 16$ is the number of modulation levels.

Fig. 2 shows the corresponding symbol-based EXIT characteristics and two "snapshot" decoding trajectories for a blocklength of $L = 10000$ 3-bit symbols, where the *a priori* information I_A is calculated by assuming independent bits for the symbol V_k. The parameter E_b is related to the energy per transmitted 16-QAM symbol E_o by $E_b = E_0/\eta$. We can observe from Fig. 2 that convergence is achieved for $E_b/N_0 = 5$ dB, which is only 1 dB away from the 16-QAM Rayleigh fading capacity evaluated at $E_b/N_0 = 4$ dB for an effective throughput of $\eta = 2$ bit/s/Hz [13, p. 751]. The bit error

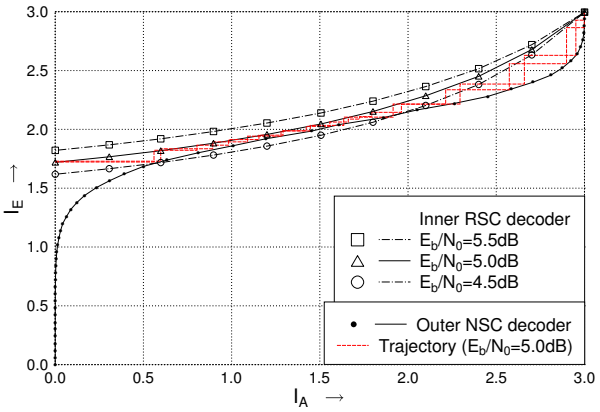

Fig. 2. EXIT chart for the NSC-RSC-16QAM BICM scheme and two "snapshot" decoding trajectories (perfectly interleaved flat Rayleigh fading channel, Gray-mapped 16-QAM, blocklength $L = 10000$ $K = 3$ bit symbols, memory-3 non-binary rate-$2/3$ outer NSC encoder and rate-$3/4$ inner RSC encoder, resp.)

rate (BER) versus E_b/N_0 performance of the NSC-RSC-16QAM BICM scheme for uncorrelated Rayleigh fading channels is displayed in Figure 3. It can be seen that the BER drops rapidly for $E_b/N_0 > 5$ dB, as the number of iterations increases. This behavior matches the predictions of the EXIT characteristics seen in Fig. 2, where the decoder becomes capable of converging for $E_b/N_0 = 5$ dB.

5.2 Turbo trellis-coded modulation

In this example a TTCM scheme combined with 16-QAM is designed for a perfectly interleaved flat

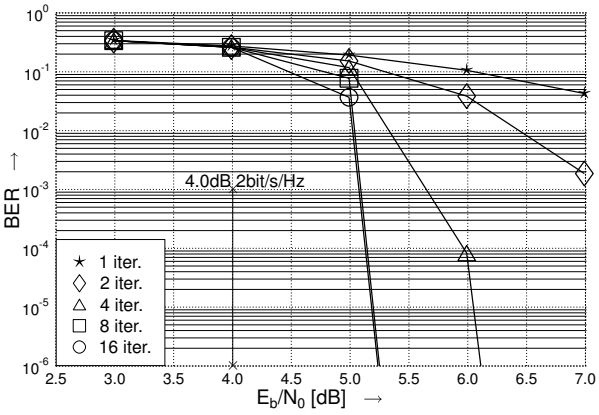

Fig. 3. BER versus E_b/N_0 on the communication channel for the NSC-RSC-16QAM BICM scheme (perfectly interleaved flat Rayleigh fading channel, Gray-mapped 16-QAM, blocklength $L = 10000$ $K = 3$ bit symbols, memory-3 non-binary rate-$2/3$ outer NSC encoder and rate-$3/4$ inner RSC encoder, resp.)

Rayleigh fading channel. As in the previous example, a code search is performed for the sake of finding the best RSC generator polynomials based on non-binary EXIT charts, where again, the complexity of a histogram-based EXIT-chart computation becomes excessive. The starting point for the code search is the memory-3 rate-$R_0 = 3/4$ RSC code having feedforward $(g_1, \ldots, g_3)$ and feedback (g_r) generator polynomials of $(g_r, g_1, g_2, g_3)_8 = (11, 2, 4, 10)_8$, which were selected from [7]. For the sake of simplicity the search was only carried out for the feedback polynomial g_r. The RSC code with $(g_r, g_1, g_2, g_3)_8 = (15, 2, 4, 10)_8$ was found to require the lowest E_b/N_0, where decoding convergence was still achievable. Analogously to the scheme proposed in [7], we employ set-partitioning based modulation [14] and a symbol-based random interleaver. As a benefit of alternately puncturing the upper and lower RSC encoded symbols in the decoder, the code rate of the TTCM scheme becomes the same as that of its constituent RSC codes, where the effective throughput of this TTCM-16QAM scheme is given by

$$\eta = R_0 \log_2(\mu) = 3 \text{ bit/s/Hz.}$$

The resultant EXIT chart, which is computed using Theorem 2 for a blocklength of $L = 100000$ 3-bit symbols is shown in Fig. 4, where the *a priori* information I_A is, again, calculated by assuming independent bits. For $E_b/N_0 = E_o/(N_0 \cdot \eta) = 8.7$ dB the iterative decoder exhibits convergence, which is only 1.1 dB away from the 16-QAM channel capacity at $E_b/N_0 = 7.6$ dB for an effective throughput of $\eta = 3$ bit/s/Hz [13, p. 751]. Fig. 5 displays the bit error rate (BER) versus the E_b/N_0 performance for transmission over the uncorrelated Rayleigh communication channel. As we can observe, the "water-fall" region appears to take shape at $E_b/N_0 > 8.7$ dB, which is consistent with the EXIT characteristics for $E_b/N_0 = 8.7$ dB seen in Fig. 4.

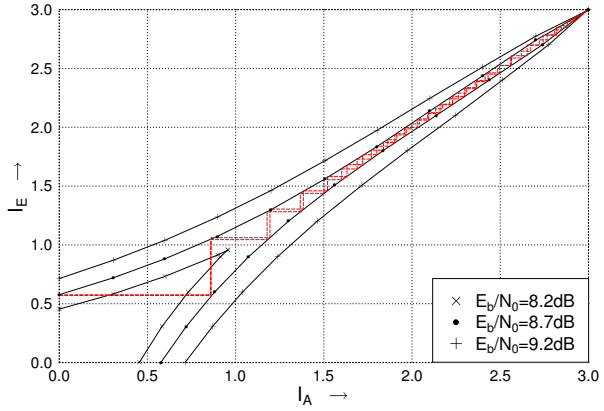

Fig. 4. EXIT chart for the TTCM-16QAM approach and two "snapshot" decoding trajectories (perfectly interleaved flat Rayleigh fading channel, blocklength 100000 symbols, signal set 16-QAM, $K = 3$, memory-3 rate-$3/4$ RSC codes)

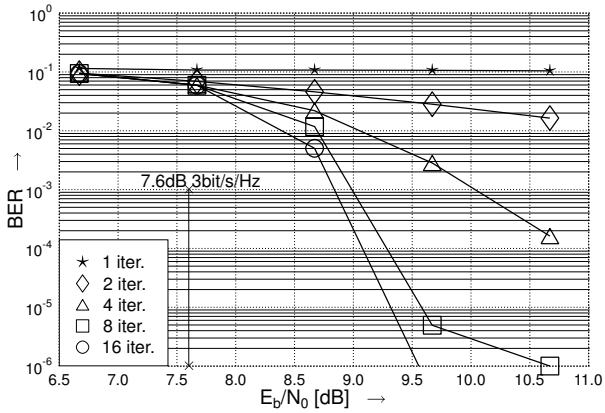

Fig. 5. Bit error rate (BER) versus E_b/N_0 on the communication channel for the TTCM-16QAM system (perfectly interleaved flat Rayleigh fading channel, blocklength 100000 symbols, signal set 16-QAM, $K = 3$, memory-3 rate-$3/4$ RSC codes)

6 Conclusions

We have derived an efficient technique for computing symbol-based EXIT charts from the extrinsic APPs for the information symbols available at the output of the constituent SISO decoders. The proposed approach exploits the recognized fact that these APPs represent a sufficient statistic for both the received sequence at the output of the communication channel and for the *a priori* information. This has been shown to hold true also for the symbol-based case. Instead of computing multidimensional histograms as in the conventional approach, we simply have to average over a function of the extrinsic APPs for a long block of data. The advantage of the proposed approach becomes particularly dominant, when the number of bits per symbol is higher than two. In this scenario the histogram-based EXIT characteristics become exceedingly difficult to compute, since their computational complexity increases exponentially with the number of bits per symbol. The proposed technique may be used for a large variety of non-binary serially and parallel concatenated systems having APP constituent decoders, as demonstrated by both the non-binary serially concatenated BICM and by the TTCM design examples provided.

Acknowledgment

The authors would like to thank Ingmar Land for fruitful discussions and Osamah R. Alamri for contributing parts of the EXIT-chart simulation software.

References

[1] S. ten Brink, "Convergence behavior of iteratively decoded parallel concatenated codes," *IEEE Trans. Comm.*, vol. 49, no. 10, pp. 1727–1737, October 2001.

[2] A. Ashikhmin, G. Kramer, and S. ten Brink, "Extrinsic information transfer functions: Model and erasure channel properties," *IEEE Trans. Inf. Theory*, vol. 50, no. 11, pp. 2657–2673, Nov. 2004.

[3] S. ten Brink, "Rate one-half code for approaching the Shannon limit by 0.1 dB," *Electron. Lett.*, vol. 36, no. 15, pp. 1293–1294, July 2000.

[4] M. Tüchler and J. Hagenauer, "Exit charts and irregular codes," in *Proc. 36th Annu. Conf. Inform. Sciences Syst*, Princeton, NJ, USA, Mar. 2002.

[5] A. Grant, "Convergence of non-binary iterative decoding," in *Proc. IEEE Global Telecommun. Conf.*, San Antonio TX, USA, Nov. 2001, pp. 1058–1062.

[6] H. Chen and A. Haimovich, "EXIT charts for turbo trellis-coded modulation," *IEEE Commun. Lett.*, vol. 8, no. 11, pp. 668–670, Nov. 2004.

[7] P. Robertson and T. Wörz, "Bandwidth-efficient turbo trellis-coded modulation using punctured component codes," *IEEE J. Sel. Areas in Commun.*, vol. 16, pp. 206–218, Feb. 1998.

[8] I. Land, P. Hoeher, and S. Gligorević, "Computation of symbol-wise mutual information in transmission systems with logAPP decoders and application to EXIT charts," in *Proc. International ITG Conference on Source and Channel Coding (SCC)*, Erlangen, Germany, Jan. 2004, pp. 195–202.

[9] J. Hagenauer, E. Offer, and L. Papke, "Iterative decoding of binary block and convolutional codes," *IEEE Trans. Inf. Theory*, vol. 42, no. 2, pp. 429–445, Mar. 1996.

[10] S. ten Brink, "Code characteristic matching for iterative decoding of serially concatenated codes," *Annals of Telecommun.*, vol. 56, no. 7-8, pp. 394–408, July-August 2001.

[11] E. Paaske, "Short binary convolutional codes with maximal free distance for rates 2/3 and 3/4," *IEEE Trans. Inf. Theory*, vol. 20, no. 5, pp. 684–689, Sept. 1974.

[12] S. Lin and D. J. Costello, *Error Control Coding: Fundamentals and Applications*, Prentice-Hall, Englewood Cliffs, New Jersey, 1983.

[13] L. Hanzo, S. X. Ng, W. T. Webb, and T. Keller, *Quadrature Amplitude Modulation: From Basics to Adaptive Trellis-Coded, Turbo-Equalised and Space-Time Coded OFDM, CDMA and MC-CDMA Systems*, John Wiley & Sons, Ltd, Chicester, 2004.

[14] G. Ungerböck, "Channel coding with multilevel/phase signals," *IEEE Trans. Inf. Theory*, vol. IT-28, no. 1, pp. 55–67, Jan. 1981.